

1 **Exo-Cleavable Linkers: A Paradigm Shift for**  
2 **Enhanced Stability and Therapeutic Efficacy in**  
3 **Antibody-Drug Conjugates**

4 **Tomohiro Watanabe<sup>†1</sup>, Naoko Arashida, Tomohiro Fujii<sup>†\*</sup>, Natsuki Shikida<sup>†</sup>, Kenichiro Ito<sup>†</sup>,**  
5 **Kazutaka Shimbo<sup>†</sup>, Takuya Seki<sup>†</sup>, Yusuke Iwai<sup>†</sup>, Ryusuke Hiramata<sup>†</sup>, Noriko Hatada<sup>†</sup>, Akira**  
6 **Nakayama<sup>†</sup>, Tatsuya Okuzumi<sup>†</sup>, Yutaka Matsuda<sup>\*‡1</sup>**

7 \* Corresponding authors

8 TF: [tomohiro.fujii.3m2@asv.ajinomoto.com](mailto:tomohiro.fujii.3m2@asv.ajinomoto.com)

9 YM: [Yutaka.Matsuda@US.AjiBio-Pharma.com](mailto:Yutaka.Matsuda@US.AjiBio-Pharma.com)

10 <sup>1</sup> These authors contributed equally.

11 <sup>†</sup>**Ajinomoto Co., Inc., 1-1, Suzuki-Cho, Kawasaki-Ku, Kawasaki-Shi, Kanagawa 210-8681, Japan.**

12 <sup>‡</sup>**Ajinomoto Bio-Pharma Services, 11040 Roselle Street, San Diego, CA 92121, United States.**

13

14

15

16

17

18

19

20 **Abstract**

21 Customized drug delivery systems have become paramount in the rapidly evolving field of precision  
22 medicine, and at the forefront of advances in this regard, antibody-drug conjugates (ADCs) present a  
23 symbiotic fusion of cytotoxic payloads and monoclonal antibodies (mAbs) facilitated by intricate chemical  
24 linkers. The search for ideal linkers that can dexterously provide the dual functionalities of enhancing  
25 circulatory stability and facilitating the effective release of the tumor payload is a present and formidable  
26 challenge. The valine-citrulline (Val-Cit) linker, which is used in a wide range of ADCs, despite its  
27 approval by the Food and Drug Administration, is associated with several inherent drawbacks, including  
28 hydrophobicity-induced aggregation, limited payload capacity, and premature payload release. This study  
29 presents a paradigm shift from the conventional linear linker archetype by introducing an exo-linker avant-  
30 garde approach that repositions the cleavable peptide linker at the exo-position of the PAB moiety. This  
31 molecular refinement not only offered the possibility to overcome the intrinsic drawbacks of the Val-Cit  
32 platform, but also significantly improved ADC stability, therapeutic efficacy, and pharmacokinetics. *In*  
33 *vitro* and *in vivo* biological evaluations, confirmed that ADCs designed using the exo-linker blueprint  
34 significantly attenuated premature payload release, while increasing the drug-to-antibody ratio, even with  
35 hydrophobic payloads, and this without inducing pronounced aggregation. Therefore, the fabricated exo-  
36 linker represents a significant improvement with respect to traditional Val-Cit ADCs. Moreover, under the  
37 influence of enzymes, such as carboxylesterases and human neutrophil elastase, the payload remained  
38 stably conjugated to the ADC, underscoring a favorable safety profile and highlighting potential for clinical  
39 translatability. Thus, our findings also demonstrate the potential of the novel exo-linker paradigm as well

40 as the profound implications of nuanced molecular modifications for reshaping ADC design and  
41 functionality.

42

43

## 44 **Introduction**

45 Recent advances in targeted therapeutics have highlighted the need for precise drug delivery to maximize  
46 therapeutic indices, while reducing systemic toxicity<sup>[1]</sup>. Central to this avant-garde paradigm is the  
47 antibody-drug conjugate (ADC), which is an intricate assembly of monoclonal antibodies (mAbs) and  
48 cytotoxic payloads<sup>[2]</sup>. This hybrid system, fabricated using specialized chemical linkers, represents a major  
49 transformation in disease intervention modalities, particularly in oncology and numerous other  
50 pathophysiological settings<sup>[3]</sup>. Further, the transformative prowess of this hybrid system is evidenced by  
51 the imprimatur of the U.S. Food and Drug Administration (FDA), which has endorsed a suite of 12 ADC  
52 entities for a range of hematological and solid malignancies. Furthermore, over 100 ADC constructs are  
53 currently undergoing rigorous clinical evaluation<sup>[1-3]</sup>.

54 The unique specificity of mAbs for targeting tumor cells is at the forefront of ADC efficacy. Notably,  
55 mAbs enhance the potency of ADCs, while expanding their therapeutic window and improving treatment  
56 durability; features that clearly superior to those of traditional chemotherapy regimens<sup>[1-3]</sup>. However, it is  
57 important to emphasize that success in such endeavors is inseparable from the selected mAb or payload.  
58 Further, the pivot point is the linker, whose architecture modulates a wide range of ADC attributes, from  
59 structural homogeneity to pharmacokinetic profiles and therapeutic safety margins, is also an important  
60 factor to consider<sup>[4]</sup>. Therefore, it is important to advance molecular acumen with respect to linker biology  
61 in realizing the potential of ADCs. Their bifunctional mandate is clear: they must exhibit molecular  
62 stability in the bloodstream and normal healthy tissue while facilitating efficient intercellular payload

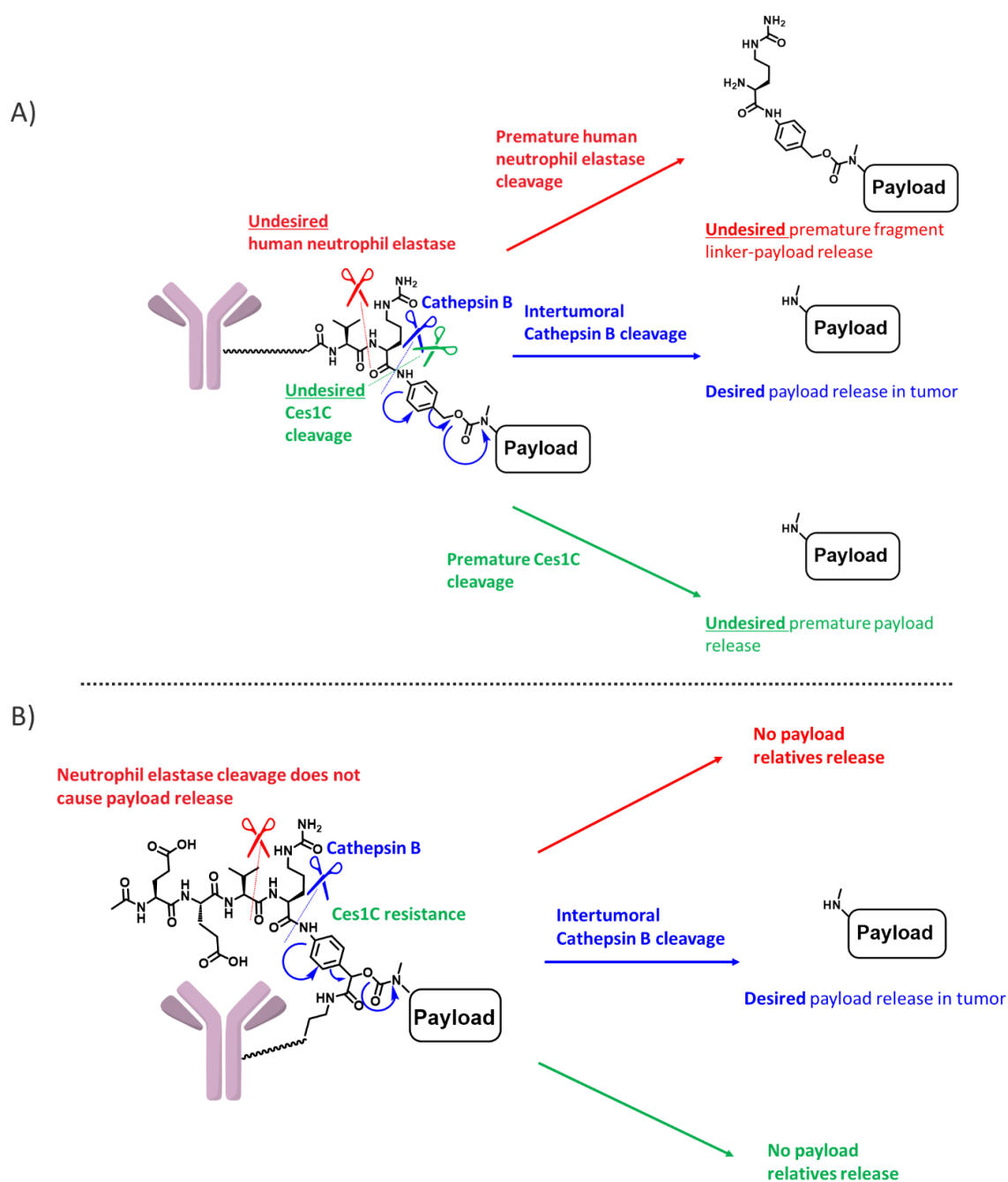
63 delivery and showing tumor-specific linker cleavage. This intricate duality has fueled fervent scientific  
64 efforts to explore the breadth and depth of linker science beyond the conventional scope of ADCs to  
65 encompass a broader spectrum of bioconjugates<sup>[5]</sup>. Paradoxically, despite the apparent proliferation of  
66 linker choices<sup>[5, 6]</sup>, there is a remarkable monotony in clinical adoption. Several FDA-approved ADCs are  
67 based on the ubiquitous Val-Cit linker or its derived Val-Ala linkers<sup>[7]</sup>.

68 The mechanism of action of Val-Cit linkers depends on cathepsin B-mediated proteolysis following ADC  
69 endocytosis by target tumor cells, and these processes ensure immediate payload release<sup>[5]</sup>. The stability  
70 of this well-established linker has been further confirmed via robust stability assays in primate and human  
71 plasma models. However, it is associated with several limitations. The intrinsic hydrophobic predilection  
72 of the Val-Cit PAB linker imposes a limit on the allowable payload amount<sup>[8]</sup>. In particular, common  
73 payload linkers, such as Mc-Val-Cit-PAB-MMAE, struggle with modest drug-antibody ratios (DAR = 3–  
74 4) and aspirations for higher ratios are thwarted by their hydrophobicity, which leads to aggregation.  
75 Additionally, insidious enzymatic interference, which leads to premature linker cleavage and subsequent  
76 payload release, further underevaluates Val-Cit chemistry. Notably, a landmark publication by Bristol  
77 Myers Squibb highlighted the vulnerability of the Val-Cit linker to carboxylesterase Ces1C, which results  
78 in premature payload detachment<sup>[9]</sup>. Moreover, Zhao et al. revealed an additional issue associated with the  
79 aberrant cleavage of the Val-Cit bond involving human neutrophil elastase, and this implies potential ADC-  
80 associated off-target toxicity, possibly leading to neutropenia<sup>[10]</sup>. Several innovative strategies for  
81 overcoming the inherent drawbacks associated with the Val-Cit platform have been developed. Most of

82 these strategies involve the use of hydrophilic polymer scaffolds, such as PEG<sup>[11]</sup>, polysarcosine<sup>[12]</sup>,  
83 cyclodextrins<sup>[13]</sup>, peptides<sup>[14]</sup>, and polyacetals<sup>[15]</sup>, which are used to mitigate payload hydrophobicity.  
84 Further, pioneering efforts by the Tsuchikama group have led to the establishment of linkers with  
85 hydrophilic moieties that exhibit recalcitrance to non-cathepsin B enzymes, with glutamic acid at the  
86 forefront<sup>[16, 17]</sup>. These novel constructs, exemplified by the Ces1C-resistant Glu-Val-Cit<sup>[6]</sup> and neutrophil  
87 elastase-resistant Glu-Gly-Cit<sup>[17]</sup> platforms herald a new era for linkers. Additionally, groundbreaking link  
88 format strategies involving tandem linkers<sup>[18]</sup>, PEG-functionalizing PAB<sup>[19]</sup>, and non-canonical amino  
89 acids have also been proposed<sup>[6]</sup>. However, these strategies have some limitations. For example, the  
90 associated synthesis processes are complex and there exists a potential impact of immunogenicity on  
91 polymer molecules<sup>[20]</sup>. Further, with respect to linear tripeptide linkers, the challenge of payload  
92 hydrophobicity still exists.

93 Therefore, in this study, we present a novel linker paradigm that offers the possibility to circumvent the  
94 intrinsic drawbacks associated with the Val-Cit linker (Figure 1). Our innovative method involves  
95 molecular recalibration, in which a canonical linear peptide-cleavable linker is repositioned at the exo  
96 position of the PAB moiety. This groundbreaking exo-linker strategy seems promising for effectively  
97 masking payload hydrophobicity by exploiting the intrinsic hydrophilicity of tetrapeptides, including Val-  
98 Cit residues. Further, this molecular metamorphosis not only confers Ces1C resistance but also  
99 circumvents human neutrophil elastase-mediated premature payload detachment. We highlight the

100 potential of our novel exo-linker and discuss how molecular finesse can be employed to redefine  
101 therapeutic paradigms.



102

103 **Figure 1.** Comparison of Val-Cit PAB and exo-cleavable linkers. (A) Val-Cit PAB linker showing desired  
104 cathepsin B cleavage and undesired cleavage mediated by Ces1C and human neutrophil elastase. (B) Exo-  
105 cleavable linker showing desired cathepsin B cleavage and undesired cleavage resistance.

106

## 107 **Results and Discussion**

### 108 **Evaluation of the physical properties of the novel exo-cleavable linkers**

109 To unravel the potential of the novel exo-linker, we performed a comparative study using a high-DAR  
110 (8) ADC alongside the traditional Val-Cit linker. Considering the inherent risk of aggregation associated  
111 with the exo-linker owing to its hydrophobic and planar structure, pyrene was chosen as the payload based  
112 on its facile synthesis process and amenability to straightforward fluorescence assays. Therefore, by  
113 leveraging a known sarcosine molecule<sup>[16]</sup>, we successfully developed a pyrene-based payload and  
114 subsequently coupled it to the exo-linker, Exo-EVC-PAB-OH. This was followed by the strategic  
115 introduction of a maleimide molecule, which culminated in the synthesis of Mal-Exo-EVC-pyrene. The  
116 detailed synthetic routes are described in the Supporting Information (Figures S1 and S2). We also  
117 synthesized Mal-Exo-EEVC-pyrene. For validation, control molecules, namely Mc-VC-PAB-pyrene and  
118 linear Mc-EVC-PAB-pyrene, were also prepared. ClogP and AlogP evaluations using a previously reported  
119 procedure<sup>[21]</sup> highlighted the distinct hydrophilicity of the exo-linker pyrenes. Using these payloads, ADCs  
120 with a DAR of 8 were synthesized via interchain-break conjugation. The fundamental work of Lyon et al.  
121 highlighted the existence of a correlation between ADC retention time during hydrophobic interaction  
122 chromatography (HIC) and systemic clearance, suggesting that accelerated retention times during HIC  
123 HPLC are indicative of favorable hydrophilic properties<sup>[22]</sup>. Notably, the significantly faster retention  
124 dynamics of trastuzumab-exo-EVC-pyrene (ADC (1)) and trastuzumab-exo-EEVC-pyrene (ADC (2))



125 relative to those of trastuzumab-VC-pyrene (ADC (3)) and trastuzumab-EVC-pyrene (ADC (4)),  
126 highlighted their hydrophilic attributes. Further, analytical findings based on size-exclusion  
127 chromatography (SEC)<sup>[23]</sup> revealed a strong disparity in aggregation, with ADC (3) and ADC (4) exhibiting  
128 pronounced aggregation, while aggregation profiles of ADC (1) and ADC (2) showed no alterations  
129 relative compared to that of native trastuzumab. In a Ces1C-enriched mouse plasma environment, the exo-  
130 linker exhibited commendable stability. The variation of the concentration of free pyrene-related  
131 compounds remained below 5% even after 4 d of incubation. This robustness was complemented by the  
132 retention of cathepsin cleavage, as described in the Supporting Information (Figure S3). Notably, even  
133 though ADC (1) and ADC (4) have nearly identical chemical formulas, subtle repositioning of the  
134 cleavable linker yielded dramatically different results. This is consistent with our preliminary hypothesis  
135 that the masking effect inherent in the cleavable peptide site, in synergy with the structural intimacy  
136 between the antibody and payload, collectively enhances ADC properties.

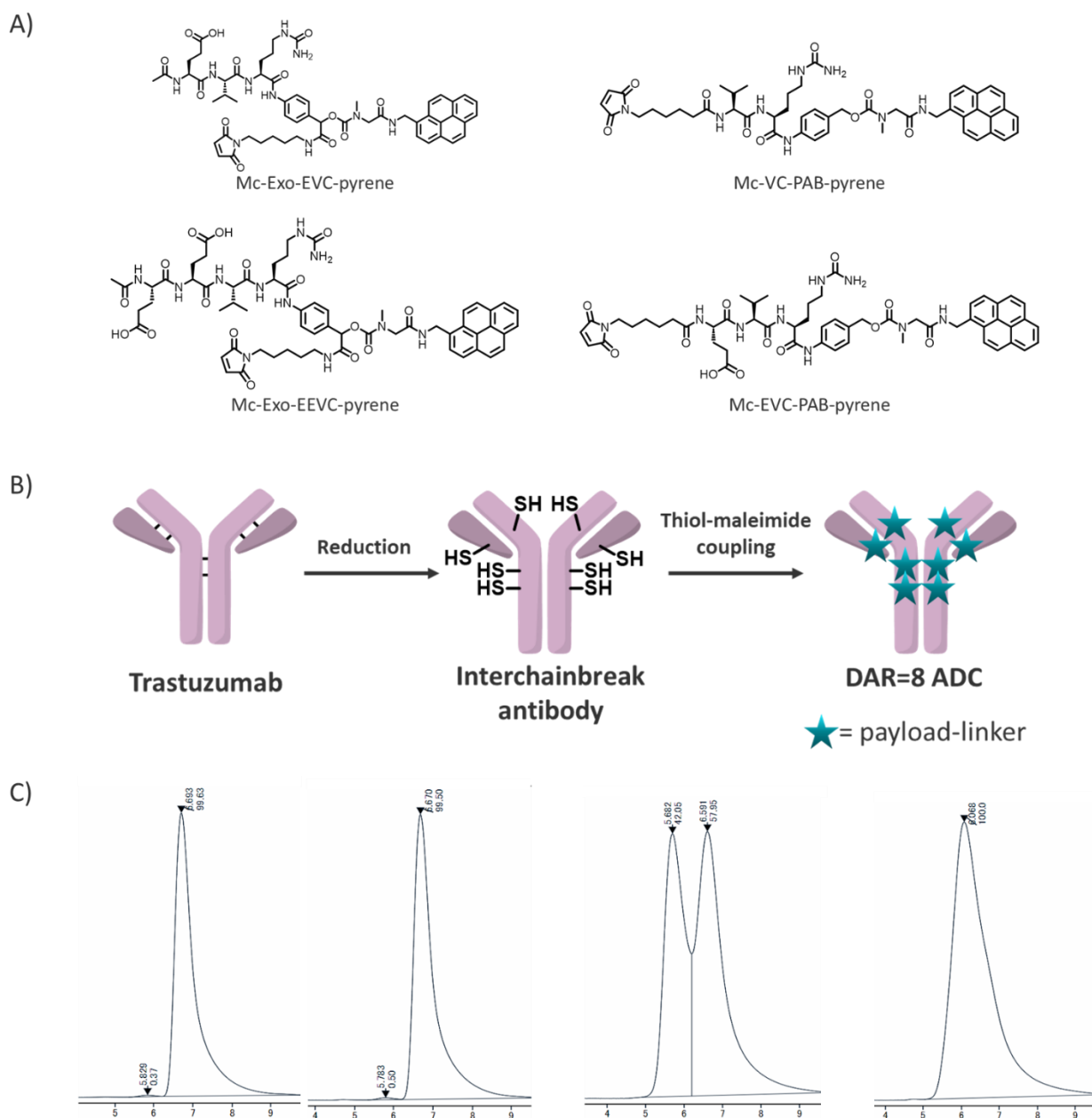


**Figure 2.** Comparison of the physical properties of Val-Cit PAB and exo-cleavable linkers. (A) Payload-linker structures. (B) Illustration of the synthesis of ADC with a DAR of 8. (C) SEC analysis of ADCs, Exo-EVC-pyrene ADC (left), Exo-EEVC-pyrene ADC (second left), EVC-pyrene ADC (second right), and VC-pyrene ADC (right).

137

138

139

140

141

142

143 **Table 1.** Summary of the comparison of the physical and mouse plasma stabilities of Val-Cit PAB and exo-  
144 cleavable linkers.

Antibody Conjugates	Linker-payload	ClogP of linker-payload	AlogP of linker-payload	HIC retention time of ADC	DAR in HIC	Aggregation in SEC	Released payload in mouse plasma
Trastuzumab	-	-	-	5.8 min	-	0.5%	-
ADC (1)	Mal-Exo-EVC-pyrene	2.21	2.06	9.7 min	8.0	0.4%	3.5%
ADC (2)	Mal-Exo-EEVC-pyrene	1.06	1.31	9.1 min	7.4	0.5%	2%
ADC (3)	Mc-VC-PAB-pyrene	4.31	3.87	15.0 min	7.9	100%	36%
ADC (4)	Mc-EVC-PAB-pyrene	3.17	3.12	14.9 min	7.8	42%	7%

145

#### 146 **Application to cytotoxic ADCs**

147 To further validate the potential of the novel exo-linker, we conjugated it with highly cytotoxic payloads,  
148 MMAE and exatecan, which are widely recognized and commonly used in commercial ADCs. Given that  
149 pyrene evaluation showed encouraging properties, our choice shifted to the exo-EEVC linker. Thus, its use  
150 lead to the synthesis of Mal-Exo-EEVC-MMAE (APL-1091) and Mal-Exo-EEVC-Exatecan (APL-1092).  
151 As recently demonstrated, site-specific conjugation tends to provide ADCs with a broader therapeutic  
152 window than their random counterparts<sup>[24, 25]</sup>. Thus, we used the second-generation AJICAP method  
153 involving an Fc affinity molecule, to selectively convert native antibodies into site-specific ADCs<sup>[26]</sup>. Thus,  
154 we generated trastuzumab by introducing a thiol group at the Lys248 site. Subsequent conjugation of the  
155 Lys248 thiol with APL-1091 and APL-1092 resulted in a targeted DAR of approximately 2 (ADC (5)):

156 APL-1091 DAR = 2; ADC (6): APL-1092 DAR = 2). Notably, both APL-1091 and APL-1092 solubilized  
157 in the conjugation buffer without the need for the addition of typical co-solvents. This highlighted the  
158 universal applicability of the *exo*-linker, even for antibodies that are potentially unstable in organic  
159 solvents. To further demonstrate the beneficial properties of the *exo*-linker, ADCs with a DAR of 8 were  
160 synthesized from both APL-1091 and APL-1092 (Figure S4; ADC (7): APL-1091 DAR = 8; ADC (8):  
161 APL-1092 DAR = 8). All these constructs exhibited acceptable HIC retention times and aggregation levels.  
162 Even though the known tendency of MMAE to aggregate was evident at a DAR of 8<sup>[27]</sup>, APL-1091 did not  
163 exhibit this tendency, confirming its hydrophilic nature.

164

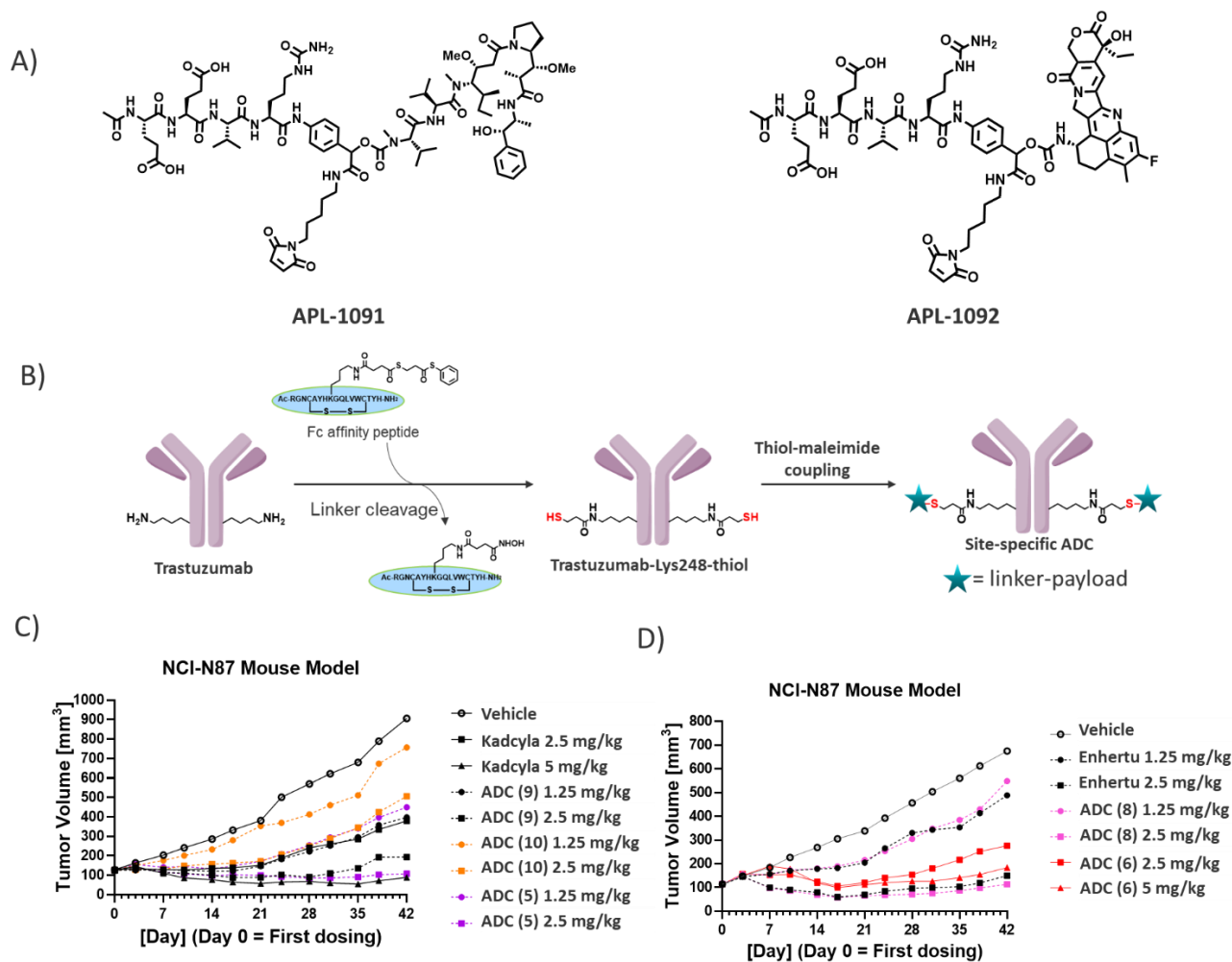
### 165 ***In vivo* xenograft studies of the novel *exo*-linker ADCs**

166 In this study, we also rigorously evaluated the fabricated ADCs using NCI-N87 xenograft mice. Thus, we  
167 were able to compare the fabricated ADCs with key industry-standard ADCs. For example, APL-1091 was  
168 comparable to a trastuzumab ADC (ADC (9)) with a DAR of 4 owing to stochastic interchain disruption,  
169 which mirrors the molecular formats of commercial ADCs, such as Adcetris and Polivy<sup>[7, 28]</sup>. Further, a  
170 site-specific ADC (ADC (10)) was designed with Mc-VC-PAB-MMAE as the payload linker using the  
171 AJICAP second-generation method in a site-specific manner<sup>[26]</sup>. This allowed for a clearer comparison of  
172 the linkers. Notably, APL-1091-based ADCs showed reasonable antitumor efficacy even at doses as low  
173 as 2.5 mg/kg, outperforming their counterparts, such as Mc-VC-PAB-MMAE-based ADCs. Even though  
174 the second-generation ADCs synthesized using AJICAP showed comparable tumor inhibition activity

175 when their payload levels were normalized, the mechanism underlying the superior efficacy of the exo-  
176 linker-based ADCs remains to be determined.

177 In a parallel study, APL-1092-based ADC was evaluated against trastuzumab-deruxtecan (Enhertu), a  
178 market-leading ADC with a DAR of 8. The dose was adjusted to match that of the payload. Thus, we  
179 observed that the ADC conjugated to APL-1092, ADC (6), showed the most pronounced antitumor activity  
180 and demonstrated substantial therapeutic efficacy at a dose of 2.5 mg/kg. Further, it showed a dose-  
181 dependent tumor-inhibitory effect on NCI-N87 cells, and when normalized to the incorporated payload  
182 amount, it showed superior tumor inhibitory effects compared to trastuzumab-deruxtecan. Furthermore,  
183 ADC (8), with a DAR of 8, analogous to trastuzumab-deruxtecan, showed significant tumor growth  
184 inhibitory effects at the tested doses, 1.25 and 2.5 mg/kg (Supporting Information, Table S1).

185 These *in vivo* efficacy studies clearly indicated that the exo-linker enhanced therapeutic efficacy owing to  
186 its increased stability in mouse plasma. This efficacy was further enhanced when the exo-linker was  
187 combined with second-generation AJICAP technologies.



188  
 189 **Figure 3.** Application to cytotoxic payloads. (A) Chemical structures of APL-1091 (Mal-Exo-EEVC-  
 190 MMAE) and APL-1092 (Mal-Exo-EEVC-Exatecan). (B) NCI-N87 *in vivo* xenograft studies of MMAE-  
 191 based ADCs, (c) NCI-N87 *in vivo* xenograft studies of Exatecan-based ADCs.

192 **Table 2.** Summary of ADCs.

Antibody Conjugates	Conjugation method	Linker-payload (payload)	ADC retention time in HIC	DAR in HIC	Aggregation in SEC
Trastuzumab	-	-	5.8 min	-	0.4%
ADC (5)	AJICAP	APL-1091 (MMAE)	8.7 min	2.0	1.4%
ADC (6)	AJICAP	APL-1092 (Exatecan)	8.0 min	2.0	1.0%
ADC (7)	Interchainbreak	APL-1091 (MMAE)	11.3 min	7.8	0.5%
ADC (8)	Interchainbreak	APL-1092 (Exatecan)	6.8 min	7.9	1.0%

ADC (9)	Interchainbreak	Mc-VC-PAB-MMAE	11.7 min	4.1	1.2%
ADC (10)	AJICAP	Mc-VC-PAB-MMAE	10.8 min	1.9	1.8%
T-DXd	Interchainbreak	Deruxtecan	9.1 min	7.8	0.1%

193

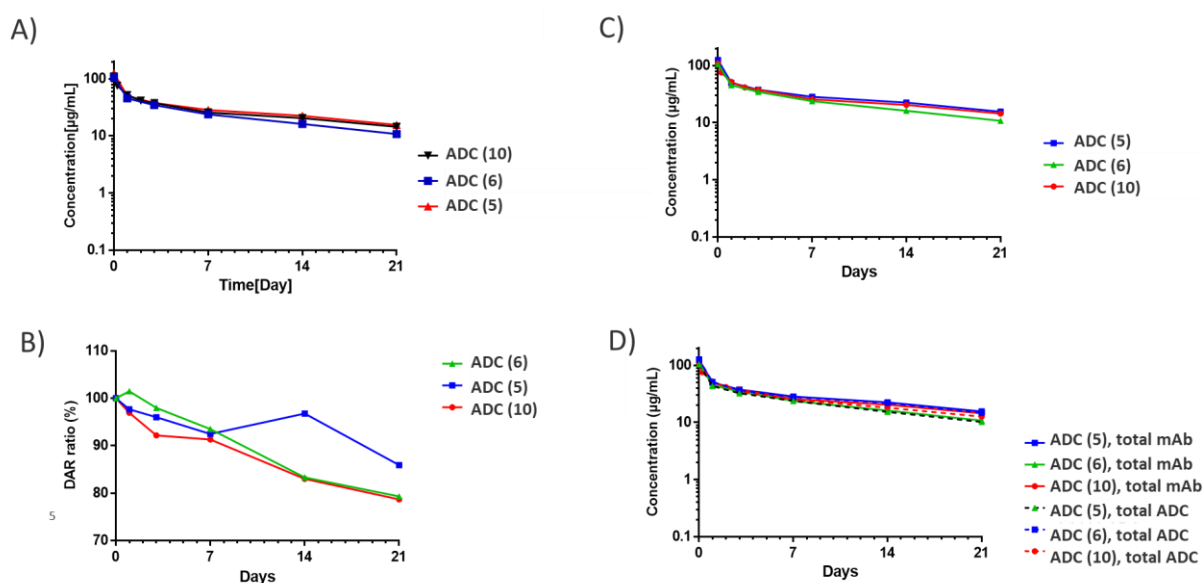
## 194 **Rat pharmacokinetics (PK) studies of the exo-linker ADCs**

195 In the field of rat PK studies, there is need for a methodological shift. Historically, the gold standard  
 196 methodology for PK studies has been the use of anti-payload antibodies via ELISA. However, the advent  
 197 of exo-linkers introduces a unique design nuance based on the ability of the linker to mask the payload.  
 198 However, this feature is associated with concerns regarding steric hindrance, which can prevent efficient  
 199 recognition by anti-payload antibodies. Therefore, to examine this concern, we performed LC-MS-based  
 200 ligand-binding assay (LBA).

201 We focused on two AJICAP site-specific ADCs, ADC (5) and ADC (6). Specifically, after dosing, blood  
 202 samples were carefully collected from the test animals using biotinylated anti-human IgG-Fc fragment-  
 203 coated beads. This was followed by an accurate LC-Q-TOF MS analysis of the samples to quantify total  
 204 ADC. The results revealed nuanced interpretations of the DAR transitions derived from the Q-TOF MS  
 205 deconvolution spectra. Interestingly, for APL-1091-based ADC (5), the DAR remained robustly high at  
 206 1.9 even on day 21. Meanwhile, APL-1092-based ADC (6) showed a decrease in DAR to 1.6 by Day 21;  
 207 however, over 80% of its payload remained integrally bound. Notably, having previously delineated the  
 208 trajectory of total ADC for ADC (10) via conventional ELISA, we sought to bridge the assay

209 methodologies. Thus, we subjected ADC (10) to LBA (Supporting Information, Figure S30). Although  
210 minor variations were observed, with slightly elevated DAR values obtained for ADC (10) via LBA, the  
211 divergence was minimal, and the peak DAR difference was only 0.2. Furthermore, a comparative analysis  
212 indicated that ADCs (5) and (6), equipped with the avant-garde exo-linker, exhibited better payload linker  
213 retention than ADC (10), with the traditional Val-Cit linker.

214 Conventional total antibody metrics were derived using a well-established anti-human antibody ELISA<sup>[25]</sup>.  
215 The scores for ADC (5) and (6) mirrored the established benchmarks set based on ADC (2) and  
216 trastuzumab. Taken together, these findings underscored the transformative stability introduced by the exo-  
217 linker in ADC design.



218

219 **Figure 4.** Pharmacokinetic Study of exo-linker-based ADCs in Rats. (A) Analysis of total antibody using  
220 ELISA. (B) Assessment of total ADC via LBA assay. (C) Trend in DAR determined based on the  
221 LBA/ELISA ratio. (D) Combined trend of total antibody and total ADC.



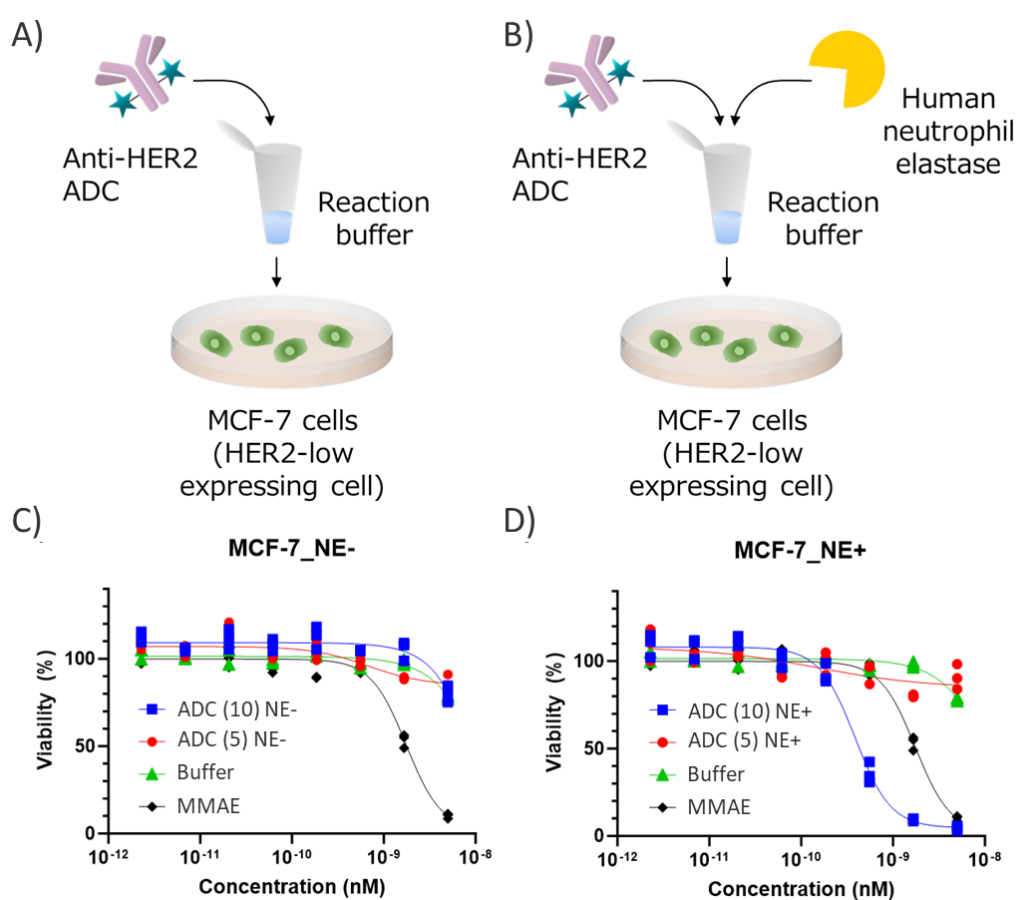
222

### 223 **In vitro human neutrophil elastase assay of exo-linker ADCs**

224 In the developing discourse regarding the Val-Cit linker, its undesired cleavage by human neutrophil  
225 elastase (NE) has emerged as a pivotal issue<sup>[10, 17]</sup>. Experimental evidence suggests that NE cleaves the  
226 peptide bond nestled between valine and citrulline in the Val-Cit linker. This enzymatic interaction triggers  
227 the conversion of the Val-Cit PAB payload to a Cit PAB payload<sup>[17, 29]</sup>, and this supposedly, results in off-  
228 target toxicity. In this study, we observed that even in the presence of NE-mediated cleavage, the exo-  
229 linker remained attached to the payload linker. This inherent robustness suggested a significant decrease  
230 in payload detachment, thereby providing protection against off-target adverse effects. Further, to test this  
231 hypothesis, an *in vitro* cytotoxicity assay was designed to detect off-target toxicity caused by NE (Figure  
232 5A and B). In this setup, ADCs with Val-Cit linkers and exo-linkers were incubated with NE, while the  
233 control ADCs, which were untreated, were incubated with model cells. In HER2-positive model cells  
234 (SKBR-3)<sup>[30]</sup>, all the ADCs with Val-Cit linkers or exo-linkers showed cytotoxicity against SKBR-3 cells  
235 regardless of NE treatment (Supplementary Figure S31). This indicated that our cell-based cytotoxicity  
236 assay was not affected by NE treatment. Next, we performed an assay using the HER2-negative MCF-7  
237 cell line. MMAE without linkers was used as a benchmark. In the NE-free environment, the potencies of  
238 all the entities, except that of MMAE, remained unchanged (Figure 5C). In contrast, in the NE-treated  
239 milieu, AC002 displayed pronounced cytotoxic attributes, exhibiting an IC<sub>50</sub> that was an order of  
240 magnitude greater than that of MMAE (Figure 5D). It has been postulated that AC002, endowed with Mc-

241 VC-PAB-MMAE, releases Cit-PAB-MMAE upon exposure to NE. The resulting Cit-PAB-MMAE,  
242 potentially driven by the hydrophobic propensity of its Cit-PAB segment, may then exhibit enhanced  
243 intracellular penetration compared to MMAE. This trend was also observed for other ADCs with Val-Cit  
244 or exo-linkers (Supplementary Figure S31), and highlighted the possibility that NE-induced off-target  
245 toxicity may have more pronounced deleterious effects than other premature payload release mechanisms,  
246 such as those driven by carboxylesterase.

247 Fortunately, the findings of this study provide compelling support that the use of the novel exo-linker offers  
248 the possibility to overcome these drawbacks. Thus, our study introduces a new era of ADCs with enhanced  
249 safety paradigms.



250

251 **Figure 5.** Evaluation of the off-target toxicity of ADCs using an *in vitro* cytotoxicity assay. (A, B)  
252 Schematic representation of the assay under (A) NE-depleted and (B) NE-pre-treated conditions. Anti-  
253 HER2 ADCs treated or not treated with NE in the NE-reaction buffer and incubated with MCF-7 cells for  
254 6 days. (C, D) Viability of cells incubated with 2.3 pM-5.0 nM of (C) Not treated and (D) NE-treated ADC  
255 (10) (blue squares), ADC (5) (red circles), MMAE (black rhombus), and blank buffer (green triangles).  
256 Individual values and fitted curves are shown based on the results of triplicate experiments.

257 The innovative introduction of exo-linkers into ADCs represents a paradigm shift in the field of ADCs as  
258 it offers the possibility to address the fundamental issues associated with traditional Val-Cit linkers. Initial  
259 comparative studies showed that ADCs synthesized using the exo-linker exhibited superior hydrophilic  
260 properties and dramatically reduced aggregation, resulting in improved systemic clearance and robust  
261 stability in Ces1C enriched mouse plasma. This superior performance was further confirmed by significant  
262 improvements in cathepsin cleavage retention. Further, the conjugation of the exo-linker with established  
263 cytotoxic payloads, namely MMAE and exatecan, enhanced its potential as evidenced by the solubility of  
264 the constructs, even in the absence of co-solvents. Furthermore, the universal applicability of the exo-  
265 linker holds promise for the design of ADCs, including those that are typically hydrophobic. This potential  
266 was further validated via *in vivo* xenograft studies, in which the exo-linker ADCs demonstrated enhanced  
267 antitumor efficacy, even at reduced doses, outperforming traditional ADCs. In particular, ADCs with APL-  
268 1091 and APL-1092 payloads showed the ability to inhibit tumor growth more effectively than leading  
269 approved ADCs when normalized for the incorporated payloads. PK studies in rats also provided insights

270 into the transformative stability conferred by the exo-linker in the ADC design. Thus, this innovative exo-  
271 linker design warrants a shift from traditional ELISAs to LC-MS-based LBAs, and demonstrates the  
272 superior performance of exo-linked ADCs in terms of payload retention relative to those with the  
273 traditional Val-Cit linker. *In vitro* assays using the exo-linker also showed resistance to NE-mediated  
274 cleavage, confirming its position as a safer alternative.

275 In summary, our results underscore the breakthrough potential of exo-linkers in revolutionizing the ADC  
276 landscape. Specifically, by offering the possibility to overcome the inherent issues associated with  
277 traditional linkers, the exo-linkers present as an avant-garde solution, ushering in a new era of ADCs  
278 characterized by improved therapeutic efficacy and safety profiles.

279

280

281 **Acknowledgments**

282 The authors wish to thank colleagues at Ajinomoto Co., Inc., and Ajinomoto Bio-Pharma Services, Inc.,  
283 for their support in the realization of this study: Dr. Tsubasa Aoki, Ms. Yumiko Suzuki, and Ms. Rika  
284 Takasugi for technical assistance with conjugations; Dr. Akira Chiba and Mr. Hiroki Imai for helpful  
285 discussions and suggestions in manuscript preparation.

286

287 **Supporting Information available.** Details of the *in vivo* studies, figures supporting exo-linker synthesis,  
288 HPLC chromatograms, and QTOF MS analyses.

289

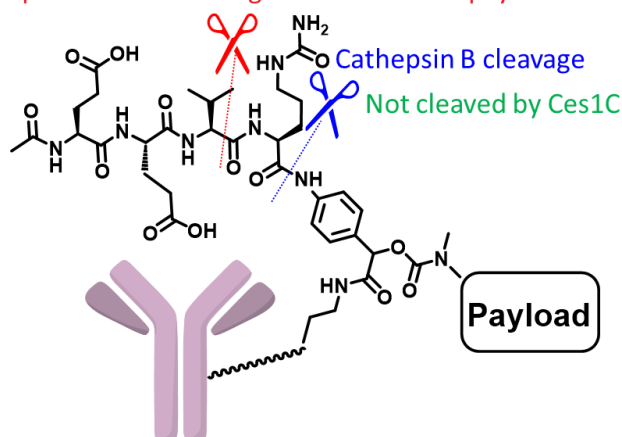
290 **Conflict of Interest**

291 This work was supported by Ajinomoto Co., Inc.

292 **Table of Contents Graphic**

## Exo-cleavable linker

Neutrophil elastase cleavage does not cause payload release



293

## 294 Synopsis

295 The authors novel drug delivery approach, refining ADCs for enhanced stability and efficacy. The  
296 introduced exo-linker outperforms traditional designs, minimizing payload issues and boosting therapeutic  
297 potential, promising improved clinical outcomes.

## 298 References

- 299 1. Qian, L.; Lin, X.; Gao, X.; Khan, R. U.; Liao, J. Y.; Du, S.; Ge, J.; Zeng, S.; Yao, S. Q. The dawn of a  
300 New Era: targeting the "Undruggables" with antibody-based therapeutics. *Chem. Rev.* **2023**, 123, 7782–  
301 7853.
- 302 2. Dumontet, C.; Reichert, J. M.; Senter, P. D.; Lambert, J. M.; Beck, A. Antibody-drug conjugates come  
303 of age in oncology. *Nat. Rev. Drug Discov.* **2023**, 22, 641–661.
- 304 3. Tarantino, P.; Ricciuti, B.; Pradhan, S. M.; Tolaney, S. M. Optimizing the safety of antibody-drug  
305 conjugates for patients with solid tumours. *Nat. Rev. Clin. Oncol.* **2023**, 20, 558–576.
- 306 4. Drago, J. Z.; Modi, S.; Chandarlapaty, S. Unlocking the potential of antibody-drug conjugates for cancer  
307 therapy. *Nat. Rev. Clin. Oncol.* **2021**, 18, 327–344.
- 308 5. Poreba, M. Protease-activated prodrugs: strategies, challenges, and future directions. *FEBS Journal*  
309 **2020**, 287, 1936–1969.
- 310 6. Wang, Z.; Li, H.; Gou, L.; Li, W.; Wang, Y. Antibody–drug conjugates: recent advances in payloads.  
311 *Acta Pharm. Sin. B* **2023**.
- 312 7. Conilh, L.; Sadilkova, L.; Viricel, W.; Dumontet, C. Payload diversification: a key step in the  
313 development of antibody-drug conjugates. *J. Hematol. Oncol.* **2023**, 16, 3.

- 314 8. Hamblett, K. J.; Senter, P. D.; Chace, D. F.; Sun, M. M.; Lenox, J.; Cervený, C. G.; Kissler, K. M.;  
315 Bernhardt, S. X.; Kopcha, A. K.; Zabinski, R. F.; Meyer, D. L.; Francisco, J. A. Effects of drug loading on  
316 the antitumor activity of a monoclonal antibody drug conjugate. *Clin. Cancer Res.* **2004**, *10*, 7063–7070.
- 317 9. Dorywalska, M.; Dushin, R.; Moine, L.; Farias, S. E.; Zhou, D.; Navaratnam, T.; Lui, V.; Hasa-Moreno,  
318 A.; Casas, M. G.; Tran, T. T.; Delaria, K.; Liu, S. H.; Foletti, D.; O'Donnell, C. J.; Pons, J.; Shelton, D. L.;  
319 Rajpal, A.; Strop, P. Molecular basis of valine-citrulline-PABC linker instability in site-specific ADCs and  
320 its mitigation by linker design. *Mol. Cancer Ther.* **2016**, *15*, 958–970.
- 321 10. Zhao, H.; Gulesserian, S.; Malinao, M. C.; Ganesan, S. K.; Song, J.; Chang, M. S.; Williams, M. M.;  
322 Zeng, Z.; Mattie, M.; Mendelsohn, B. A.; Stover, D. R.; Doñate, F. A potential mechanism for ADC-  
323 induced neutropenia: role of neutrophils in their own demise. *Mol. Cancer Ther.* **2017**, *16*, 1866–1876.
- 324 11. Giese, M.; Davis, P. D.; Woodman, R. H.; Hermanson, G.; Pokora, A.; Vermillion, M. Linker  
325 architectures as steric auxiliaries for altering enzyme-mediated payload release from bioconjugates.  
326 *Bioconjug. Chem.* **2021**, *32*, 2257–2267.
- 327 12. Viricel, W.; Fournet, G.; Beaumel, S.; Perrial, E.; Papot, S.; Dumontet, C.; Joseph, B. Monodisperse  
328 polysarcosine-based highly-loaded antibody-drug conjugates. *Chem. Sci.* **2019**, *10*, 4048–4053.
- 329 13. Evans, N.; Grygorash, R.; Williams, P.; Kyle, A.; Kantner, T.; Pathak, R.; Sheng, X.; Simoes, F.;  
330 Makwana, H.; Resende, R.; de Juan, E.; Jenkins, A.; Morris, D.; Michelet, A.; Jewitt, F.; Rudge, F.; Camper,  
331 N.; Manin, A.; McDowell, W.; Pabst, M.; Godwin, A.; Frigerio, M.; Bird, M. Incorporation of hydrophilic  
332 macrocycles into drug-linker reagents produces antibody-drug conjugates with enhanced in vivo  
333 performance. *Front. Pharmacol.* **2022**, *13*, 764540.
- 334 14. Haeckel, A.; Appler, F.; Ariza de Schellenberger, A.; Schellenberger, E. XTEN as biological alternative  
335 to pegylation allows complete expression of a protease-activatable Killin-based cytostatic. *PLOS ONE*  
336 **2016**, *11*, e0157193.
- 337 15. Toader, D.; Fessler, S. P.; Collins, S. D.; Conlon, P. R.; Bollu, R.; Catcott, K. C.; Chin, C. N.; Dirksen,  
338 A.; Du, B.; Duvall, J. R.; Higgins, S.; Kozytska, M. V.; Bellovoda, K.; Faircloth, C.; Lee, D.; Li, F.; Qin,  
339 L.; Routhier, C.; Shaw, P.; Stevenson, C. A.; Wang, J.; Wongthida, P.; Ter-Ovanesyan, E.; Ditty, E.; Bradley,  
340 S. P.; Xu, L.; Yin, M.; Yurkovetskiy, A. V.; Mosher, R.; Damelin, M.; Lowinger, T. B. Discovery and  
341 preclinical characterization of XMT-1660, an optimized B7-H4-targeted antibody-drug conjugate for the  
342 treatment of cancer. *Mol. Cancer Ther.* **2023**, *22*, 999–1012.
- 343 16. Anami, Y.; Yamazaki, C. M.; Xiong, W.; Gui, X.; Zhang, N.; An, Z.; Tsuchikama, K. Glutamic acid-  
344 valine-citrulline linkers ensure stability and efficacy of antibody-drug conjugates in mice. *Nat. Commun.*  
345 **2018**, *9*, 2512.
- 346 17. Ha, S. Y. Y.; Anami, Y.; Yamazaki, C. M.; Xiong, W.; Haase, C. M.; Olson, S. D.; Lee, J.; Ueno, N. T.;  
347 Zhang, N.; An, Z.; Tsuchikama, K. An enzymatically cleavable tripeptide linker for maximizing the  
348 therapeutic index of antibody-drug conjugates. *Mol. Cancer Ther.* **2022**, *21*, 1449–1461.
- 349 18. Chuprakov, S.; Ogunkoya, A. O.; Barfield, R. M.; Bauzon, M.; Hickie, C.; Kim, Y. C.; Yeo, D.; Zhang,  
350 F.; Rabuka, D.; Drake, P. M. Tandem-cleavage linkers improve the in vivo stability and tolerability of  
351 antibody-drug conjugates. *Bioconjug. Chem.* **2021**, *32*, 746–754.

- 352 19. Poudel, Y. B.; Chowdari, N. S.; Cheng, H.; Iwuagwu, C. I.; King, H. D.; Kotapati, S.; Passmore, D.;  
353 Rampulla, R.; Mathur, A.; Vite, G.; Gangwar, S. Chemical modification of linkers provides stable linker-  
354 payloads for the generation of antibody-drug conjugates. *ACS Med. Chem. Lett.* **2020**, *11*, 2190–2194.
- 355 20. Garay, R. P.; El-Gewely, R.; Armstrong, J. K.; Garratty, G.; Richette, P. Antibodies against polyethylene  
356 glycol in healthy subjects and in patients treated with PEG-conjugated agents. *Expert Opin. Drug Deliv.*  
357 **2012**, *9*, 1319–1323.
- 358 21. Fujii, T.; Reiling, C.; Quinn, C.; Kliman, M.; Mendelsohn, B. A.; Matsuda, Y. Physical characteristics  
359 comparison between maytansinoid-based and auristatin-based antibody-drug conjugates. *Explor. Target*  
360 *Antitumor Ther.* **2021**, *2*, 576–585.
- 361 22. Lyon, R. P.; Bovee, T. D.; Doronina, S. O.; Burke, P. J.; Hunter, J. H.; Neff-LaFord, H. D.; Jonas, M.;  
362 Anderson, M. E.; Setter, J. R.; Senter, P. D. Reducing hydrophobicity of homogeneous antibody-drug  
363 conjugates improves pharmacokinetics and therapeutic index. *Nat. Biotechnol.* **2015**, *33*, 733–735.
- 364 23. Nakahara, Y.; Mendelsohn, B. A.; Matsuda, Y. Antibody–drug conjugate synthesis using continuous  
365 flow microreactor technology. *Org. Process Res. Dev.* **2022**, *26*, 2766–2770.
- 366 24. Zhou, Q. Site-specific antibody conjugation with payloads beyond cytotoxins. *Molecules* **2023**, *28*.
- 367 25. Matsuda, Y.; Seki, T.; Yamada, K.; Ooba, Y.; Takahashi, K.; Fujii, T.; Kawaguchi, S.; Narita, T.;  
368 Nakayama, A.; Kitahara, Y.; Mendelsohn, B. A.; Okuzumi, T. Chemical site-specific conjugation platform  
369 to improve the pharmacokinetics and therapeutic index of antibody-drug conjugates. *Mol. Pharm.* **2021**,  
370 *18*, 4058–4066.
- 371 26. Fujii, T.; Matsuda, Y.; Seki, T.; Shikida, N.; Iwai, Y.; Ooba, Y.; Takahashi, K.; Isokawa, M.; Kawaguchi,  
372 S.; Hatada, N.; Watanabe, T.; Takasugi, R.; Nakayama, A.; Shimbo, K.; Mendelsohn, B. A.; Okuzumi, T.;  
373 Yamada, K. AJICAP second generation: improved chemical site-specific conjugation technology for  
374 antibody-drug conjugate production. *Bioconjug. Chem.* **2023**, *34*, 728–738.
- 375 27. Satomaa, T.; Pynnönen, H.; Vilkmann, A.; Kotiranta, T.; Pitkänen, V.; Heiskanen, A.; Herpers, B.; Price,  
376 L. S.; Helin, J.; Saarinen, J. Hydrophilic auristatin glycoside payload enables improved antibody-drug  
377 conjugate efficacy and biocompatibility. *Antibodies (Basel)* **2018**, *7*.
- 378 28. Matsuda, Y.; Leung, M.; Tawfiq, Z.; Fujii, T.; Mendelsohn, B. A. In-situ reverse phased HPLC analysis  
379 of intact antibody-drug conjugates. *Anal. Sci.* **2021**, *37*, 1171–1176.
- 380 29. Miller, J. T.; Vitro, C. N.; Fang, S.; Benjamin, S. R.; Tumey, L. N. Enzyme-agnostic lysosomal screen  
381 identifies new legumain-cleavable ADC linkers. *Bioconjug. Chem.* **2021**, *32*, 842–858.
- 382 30. Ogitani, Y.; Aida, T.; Hagihara, K.; Yamaguchi, J.; Ishii, C.; Harada, N.; Soma, M.; Okamoto, H.; Oitate,  
383 M.; Arakawa, S.; Hirai, T.; Atsumi, R.; Nakada, T.; Hayakawa, I.; Abe, Y.; Agatsuma, T. DS-8201a, A novel  
384 HER2-targeting ADC with a novel DNA topoisomerase I inhibitor, demonstrates a promising antitumor  
385 efficacy with differentiation from T-DM1. *Clin. Cancer Res.* **2016**, *22*, 5097–5108.

386

387